Ebrahim, Neven A. and Leach, Lopa (2015) Temporal studies into attachment, VE-cadherin perturbation, and paracellular migration of human umbilical mesenchymal stem cells across umbilical vein endothelial monolayers. Stem Cells and Development, 24 (4). pp. 426-436. ISSN 1547-3287

STEM CELLS AND DEVELOPMENT
Volume 00, Number 00, 2014

DOI: 10.1089/scd.2014.0207

ORIGINAL RESEARCH REPORT

Temporal Studies into Attachment, Vascular Endothelial-Cadherin Perturbation, and Paracellular Migration of Human Umbilical Mesenchymal Stem Cells Across Umbilical Vein Endothelial Monolayers

Neven A. Ebrahim and Lopa Leach

Mesenchymal stem cells from Wharton's jelly of human umbilical cords (WJ-MSC) are a valuable alternate source of stem cells. Their role in situ and whether they can interact and cross intact endothelial monolayers requires elucidation. The aim of this study was to investigate the dynamic interactions between WJ-MSC and human umbilical vein endothelial cells (HUVEC), including attachment, transit times, extravasation pathway, and the effects of WJ-MSC on junctional vascular endothelial (VE)-cadherin. HUVEC were grown to near confluence in endothelial media and to full confluence in mixed media before the addition of PKH26-labelled WJ-MSC. Time lapse fluorescence microscopy showed stem cells undergoing membrane blebbing followed by amoeboid movement on HUVEC monolayers before rounding up and changing shape toward the spindle-shaped morphology during/after transmigration to subendothelial positions. Cells demonstrated a time lag of 60 min before paracellular extravasation, confirmed by confocal microscopy. Forty-six percent of attached cells crossed in the first 2 h. By 16 h, a majority of cells had transmigrated with >96% of cells crossing by 22 h. There were concomitant changes in endothelial junctional VE-cadherin with statistically significant increases in discontinuous staining at 2 h, return to control values at 16 h, even as from 22 h onward HUVEC displayed increased percentage of junctions with continuous staining and upregulation of protein. Our data suggests that WJ-MSC crosses the endothelial barrier through the paracellular pathway and can influence junctional organization of HUVEC with discreet perturbation of VE-cadherin preceding transmigration followed by upregulation once the adluminal side is reached. The latter may reflect a perivascular support function of WJ-MSC in the umbilical cord.

Introduction

The Wharton's jelly (WJ) of the umbilical cord is derived from the mesoderm of the primitive streak, which invades the connecting stalk and primary chorionic villi early in gestation. Mesenchymal stem cells (MSC) of the mesoderm differentiate into and participate in neovasculogenesis of both the umbilical and placental circulation. The WJ at term continues to encase the fetal umbilical vein and arteries (two) and still contain multipotent MSCs [1]. The role of these cells throughout gestation is not known, although paracrine cross-talk may be important for vessel growth, maturation, and function. MSCs from the umbilical cord can be easily isolated after parturition. Their phenotype is similar to adult bone marrow stem cells, but being fetal they have the added advantage of advanced potency and less immunogenicity than adult stem cells [2]. This makes them an attractive source for future stem cell therapy, although their fundamental biology still remains underresearched.

Currently, a large number of clinical trials are underway evaluating adult bone marrow-derived MSCs (BM-MSCs) for the treatment of cardiovascular, inflammatory, and autoimmune diseases. Most involve systemic infusion of MSC into the vascular circulation [3] and thus cells have to extravasate to target areas. In vitro studies have shown that MSC transmigrate, similar to leukocytes, through predominantly paracellular and also transcellular pathways in activated endothelium [4]. The authors reported that the initiation of transmigration occurred by 30 min with 50% of stem cells completing transmigration after 120 min. Using an isolated murine heart perfusion system, Schmidt et al. [5] have shown that MSC transmigrate through the paracellular

Cardiovascular Research Group, School of Life Sciences, Faculty of Medicine & Health Sciences, University of Nottingham, Nottingham, United Kingdom.

junctions, with one third of the cells migrating within 30 min, suggestive of a faster transit time in vivo. Whether WJ-MSC uses the paracellular route and the duration of attachment and transmigration events is not known and is the central aim of this study.

In most non-CNS vascular beds, paracellular permeability is regulated in a dynamic manner by adherens junctions (AJs), with vascular endothelial (VE)-cadherin being the key player [6]. Phosphorylation of VE-cadherin and loss of anchorage leads to translocation of this molecule from adherens junctional domains and accompanying increased paracellular permeability to hydrophilic solutes and extravasating blood cells [5]. In the endothelium with tighter barriers, such as the blood–brain barrier, tight junctions also regulate the paracellular passage of cells, molecules, and ions. Human umbilical vein endothelial cells (HUVEC) are a useful and favored in vitro model for endothelial barrier studies and are easily isolated from the umbilical cord. The close proximity between the WJ-MSC and the umbilical vein endothelial cells in situ and their developmental origins makes the use of HUVEC doubly pertinent for this study. Using real-time fluorescence microscopy and confocal scanning microscopy, the cellular mechanisms used in the attachment and transmigration of WJ-MSC across HUVEC monolayers, the time taken, and the associated dynamics of the junctional VE-cadherin was, therefore, investigated. Data obtained may also reveal the importance of paracrine cross talk between umbilical stem cells and blood vessels for the continued maintenance of endothelial integrity during gestation.

Materials and Methods

Isolation and culture of cells

Term umbilical cords ($n = 20$) were obtained at elective Cesarean section from normal pregnancies with informed patient consent, full ethical approval (REC Ref 14/SC/1194, NHS Heath Research Authority), and NHS permission from Nottingham University Hospitals, NHS Trust, UK. WJ-MSC were non-enzymatically isolated using the method of De Bruyn et al. [7]. WJ-MSC migrating from umbilical cord segments on plastic Petri dishes were cultured in a stem cell growth medium [DMEM/Low Glucose (Hyclone) with 15% fetal bovine serum (FBS; Sigma) and antibiotic/antimycotic solution (Hyclone)]. They were characterized according to the Mesenchymal and Tissue Stem Cell Committee of the International Society for Cellular Therapy [8] by flow cytometry FC 500 (Beckman Coulter) with 50,000 events captured. Results were analyzed using the WEASEL v3.0 for Windows (Walter and Eliza Hall Institute). The ability to differentiate into adipocytes, chondrocytes (according to Pittenger et al. [9]), and osteocytes (according to Santos et al. [10]) was verified. Endothelial cells (HUVEC) were isolated from freshly collected term umbilical cords using the method of Hamilton and Leach [11]. They were grown up to passage 3 on gelatin-coated flasks and were maintained in endothelial medium [Medium 199 (Gibco) with 20% FBS + heparin sodium salt (50 μg/mL), endothelial cell growth supplement (50 μg/mL)]. The endothelial specific cell–cell adhesion molecule, VE-cadherin (Pharmingen, BD Biosciences) and von Willebrand Factor (vWF; Dako) was used to check the junctional maturity and homogeneity of HUVEC.

Effect of mixed media on the cells

Before the coculture study, the ability of HUVEC to attach and grow to confluence in mixed endothelial and stem cell growth media (50% endothelial medium + 50% stem cell medium) was ascertained by microscopical observations. Changes, if any, of the endothelial markers VE-cadherin and vWF in HUVEC was investigated by immunocytochemistry (see Immunohistochemistry section below). WJ-MSC at passage 3, 4, and 5 were labeled with PKH26 fluorescent dye (Sigma-Aldrich) according to the manufacturer's instructions. Similarly, the ability of labeled WJ-MSC to attach, grow, and proliferate on 1% gelatin in mixed media was also investigated. WJ-MSC were cultured at an initial cell density of 64 cells/mm^2 for 22 h. The attached cells were photographed and 10 unbiased images were taken for the 2, 16, and 22 h groups (three experimental repeats) using phase contrast microscopy. Every second image was selected from each group and the number of cells counted. The mean number of cells/mm^2 was calculated. The labeled WJ-MSC were also subjected to immunocytochemistry to localize any VE-cadherin expression in mixed media.

Coculture studies

To obtain cocultures of HUVEC in contact with WJ-MSC, 100,000 HUVEC were seeded on a 1% gelatin-coated coverslip (19 mm diameter) and incubated in endothelial media (three different isolates were tested, with three experimental repeats). Once 70% confluence was reached, the media was changed to mixed media. On full confluence (18–24 h later) 20,000 labeled WJ-MSC were seeded on top of the confluent HUVEC monolayer (1:5 ratio) per coverslip in 1 mL of the mixed media [12]. HUVEC monolayers without added WJ-MSC in mixed media were used as a control. WJ–MSC–HUVEC interaction was observed at different time intervals (2, 4, 6, 22, and 26 h) by an inverted phase microscope and photographed.

Real time observations

Cocultures of WJ-MSC on HUVEC on glass-bottomed tissue culture dishes (Ibidi GmBH) were observed with DMIRE2 time-lapse fluorescent microscope with a built-in environmental chamber and a color CCD camera (Leica DC300FX) and also with a wide-field fluorescence microscope (Deltavision Elite; Applied Precision). Cells were observed for 40 h. All data analyses were carried out using the Volocity software (Perkin Elmer).

Immunohistochemistry of VE-cadherin and systematic random sampling

To localize VE-cadherin in HUVEC and monitor the effects of labeled WJ-MSC on VE-cadherin, cocultured cells were fixed with 1% paraformaldehyde, pH 7.3 at different time intervals (2, 4, 6, 12, 14, 16, 22, and 26 h). They were permeabilized for 10 min with 0.15% Triton X-100, blocked in 5% goat's serum in phosphate buffered saline (PBS) for 30 min and incubated overnight at 4°C with mouse anti-Human CD144 (VE-cadherin; 5 μg/mL). Cells were washed with 0.1% PBS/BSA and incubated with FITC-conjugated goat anti-mouse IgG (Sigma) for 2 h in the dark at room temperature (RT). The

coverslips were mounted using Vectorshield. They were analyzed using a Nikon fluorescence microscope with appropriate filters to allow visualization of both FITC and PKH26. Localization and continuous/discontinuous staining pattern of endothelial cell–cell junctions and position of labeled WJ-MSC was photographed with the CCD camera (Nikon DS) for the chosen intervals of coculture and stored (NIS elements F3.0; Nikon). HUVEC alone and labeled WJ-MSC alone for similar durations of culture in mixed media were also subjected to VE-cadherin immunocytochemistry to obtain appropriate controls.

Junctional counts

Stored Images (duration of coculture was blinded) were used to count the percentage of paracellular clefts showing continuous or discontinuous (disrupted) VE-cadherin staining in control and treated HUVEC monolayers. To ensure that all cell–cell junctional regions had an equal chance of being counted, a grid was placed on images and paracellular clefts from every other square were counted and categorized according to staining pattern. The position and number of the labeled WJ-MSC, apical, or sub-endothelial and their proximity to discontinuous junctions were recorded for the cocultures.

Statistical analysis

Data were analyzed using the two-way ANOVA (Prism 6 software) and Bonferroni's multiple comparison test to compare control versus stem cell treated group at 2, 16, and 22 h. Tukey's multiple comparison test was used to compare controls alone and cocultures alone at the same time intervals. Statistical significance was taken at $P < 0.05$.

Confocal imaging

Immunocytochemically labeled cocultures at 2 and 22 h were further analyzed with confocal scanning microscopy (Zeiss Axiovision; Zeiss) and the Zen 2009 software for multichannel acquisition and image processing. The pinhole diameter used in all confocal imaging was 1 airy unit. Optical slices (0.5–0.6 μm intervals) were taken and Z-tilts were obtained to visualize transmigration pathways.

Western blotting

Confluent HUVEC monolayers were cocultured with or without WJ-MSC (1:5 ratio). The early hours of interaction (0, 2 h) and late (22 h) were chosen to measure VE-cadherin protein levels. WJ-MSC alone was grown in mixed media on gelatin and cells at 0, 2, and 22 h were used for immunoblotting. Briefly, cells were scraped and lysed in a 200 μL Lysis buffer [20 mM Tris (Invitrogen) + 320 mM sucrose (BDH) + 0.1% Triton X-100 + 1 mM NaF + 10 mM β glycerophoshate + 1 mM EGTA and protease inhibitor; pH 7.6]. Denatured proteins were separated in a 4%–20% gradient polyacrylamide gel after equal loading (15 μL) and

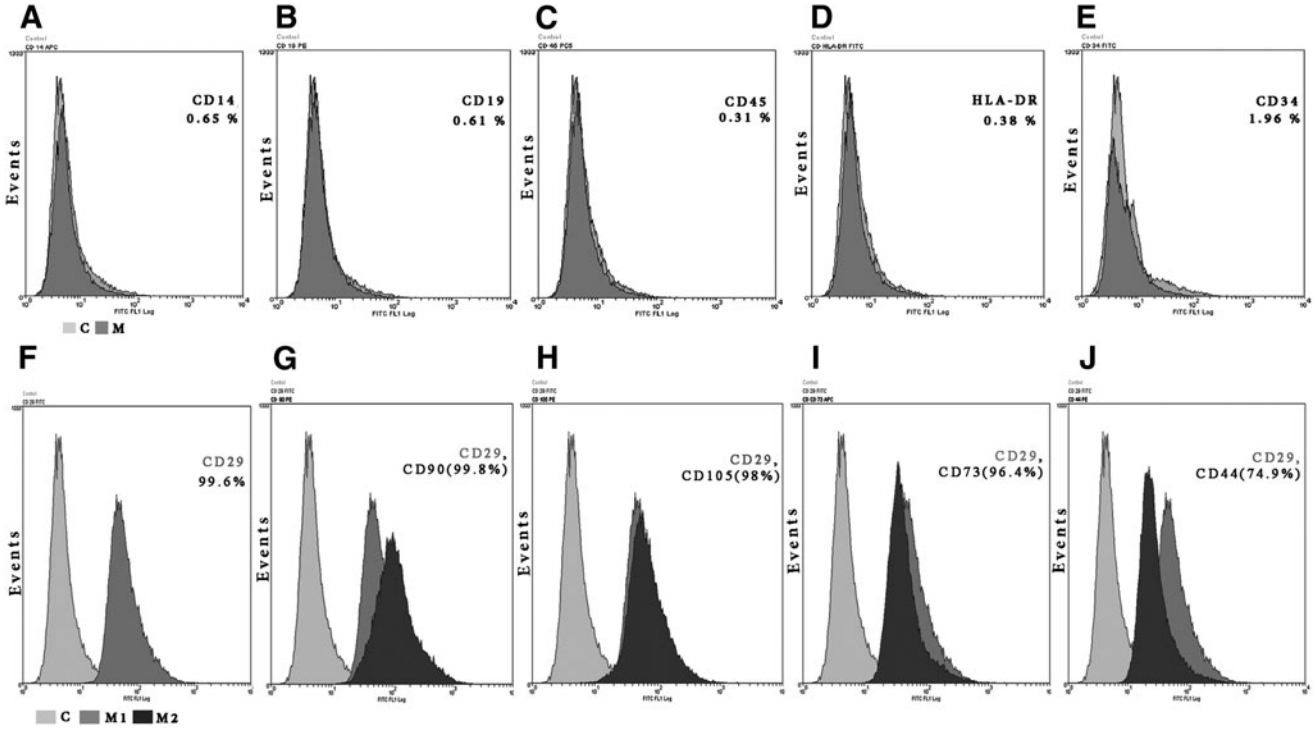

FIG. 1. Flow cytometric analysis of WJ-MSC (P3) for hematopoietic **(A–E)** and MSC surface markers **(F–J)**. **(A–E)** The *dark gray histograms* (M) represent cells labeled with hematopoietic markers; *light gray* (C) are control; percentages indicate the labeled marker rates. Less than 2% of WJ-MSC are immunopositive to the hematopoietic markers CD14, CD19, CD45CD, HLA-DR, and CD 34. **(F–J)** The *dark gray* (M1) represents CD29 and the *black* (M2) represents CD90, CD105, CD73, and CD44 respectively; *light gray histograms* (C) are negative control. Greater than 96% show immunopositivity to the mesenchymal markers CD 29, CD90, CD105, and CD73 and 74.9% were positive to CD44. WJ-MSC from all passages used (before and after freezing) showed similar profiles. WJ-MSC, mesenchymal stem cells from Wharton's jelly of human umbilical cords.

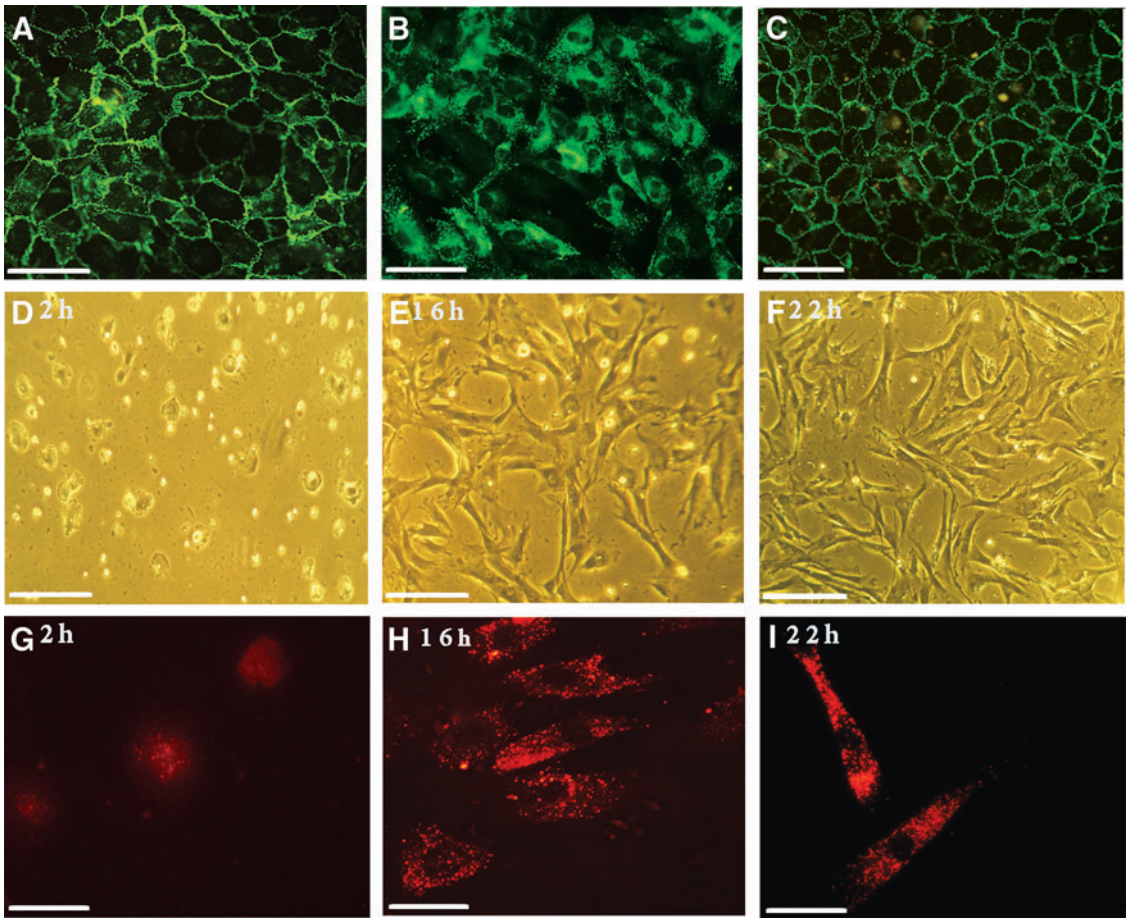

FIG. 2. **(A–C)** Immunofluorescence analyses of HUVEC grown in endothelial medium **(A, B)** versus mixed media **(C)**. VE-cadherin is localized to cell–cell boundaries and display a predominantly continuous staining whereas punctate vWF staining is found in the cytoplasm. A similar continuous pattern of VE-cadherin can be seen in mixed media; Bar = 40 μm. **(D–I)** Images of PKH26-labeled WJ-MSC in mixed media on 1% gelatin-coated coverslips at 2, 16, and 22 h. Phase contrast images **(D–F)** show attachment, change in morphology toward the elongated spindle-shape and increasing confluence with time, Bar = 200 μm. Fluorescence micrographs **(G–I)** of labeled WJ-MSC (*red*) immunostained for VE-cadherin (*green*). Cells are immunonegative at each duration; Bar = 40 μm. HUVEC, human umbilical vein endothelial cells; VE, vascular endothelial; vWF, von Willebrand Factor. Color images available online at www.liebertpub.com/scd

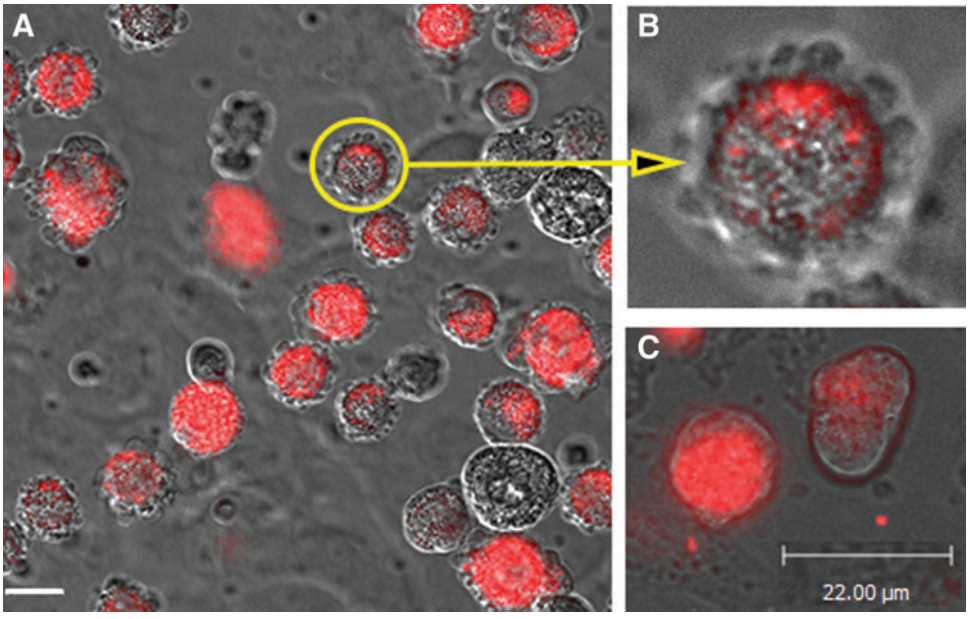

FIG. 3. **(A, B)** Micrographs from time lapse photography (0–2 h) showing blebbing phenomenon of all PKH26-labeled WJ-MSC when added to HUVEC monolayer. Bar = 6 μm. **(B)** A higher magnification of A (×2.5) of one cell (*circle* and *arrow*). **(C)** Micrograph from time-lapse photography showing shedding of PKH26-labeled exosomes from WJ-MSC overlying HUVEC; Bar = 22 μm. Color images available online at www.liebertpub.com/scd

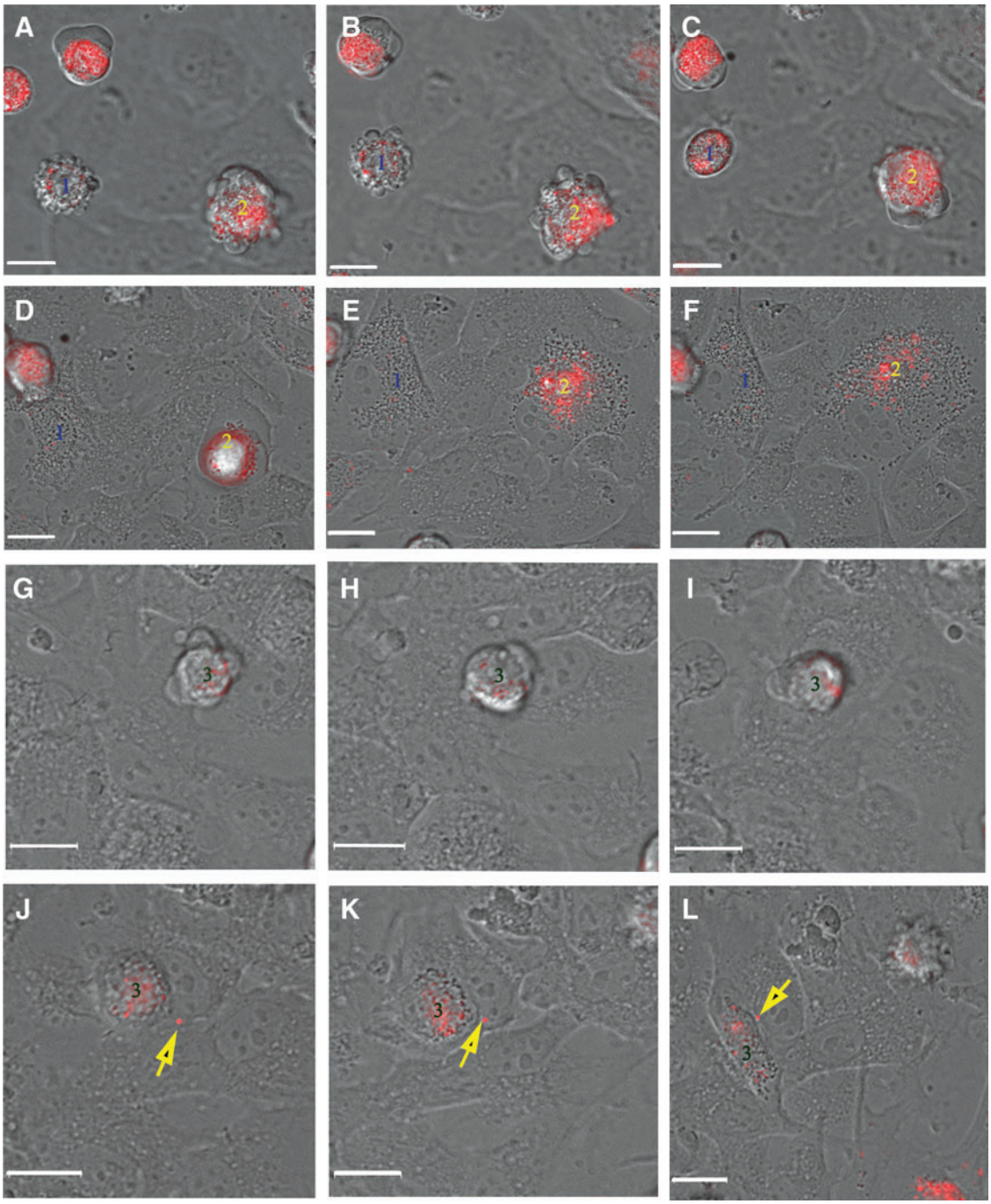

FIG. 4. **(A–F)** Micrographs from time-lapse photography (every 15 min for 1.5 h) showing behavior of labeled WJ-MSC over HUVEC monolayers. Cell 1 can be seen displaying blebbing behavior **(A, B)** followed by rounding (after 30 min; **C**), and flattening **(D–F)**. Cell 2 can be seen blebbing **(A, B)**, crawling **(C)**, rounding **(D)**, and flattening **(E, F)**. **(G–L)** Micrographs from a second time-lapse movie (every 15 min for 1.5 h). Cell 3 can be seen demonstrating pseudopodia and crawling movement over HUVEC monolayer **(G–I)**, rounding **(J, K)** before becoming spindle shaped **(L)**. From **(A–C)** micrographs were focused on WJ-MSC, whereas micrographs from **(D–L)** were focused on HUVEC. WJ-MSC have not crossed the HUVEC monolayer in these micrographs of early events. Secreted PKH26-labeled exosome (*yellow arrow*) can be seen in **(J)**, **(K)**, and **(L)**. Bar = 6 μm. Color images available online at www.liebertpub.com/scd

transferred to a nitrocellulose membrane. After blocking with 5% skimmed milk powder in 0.1% Tris buffered saline with Tween 20 for 60 min at RT, the membranes were incubated with the antibodies against VE-cadherin (1:1,000 dilution; Cell Signalling) and GAPDH (1:3,000; Sigma). A Li-cor Odyssey scanner and Odyssey software (Image Studio Version 3.1.4) were used to measure optical densities. The VE-cadherin protein expression (normalized using GAPDH as loading control) for the different durations and study groups (three experimental repeats) were obtained. Data

were analyzed using two-way ANOVA and Sidak's multiple comparison test. Statistical significance was taken at $P < 0.05$.

Results

Characterization of isolated WJ-MSC and HUVEC

Under our laboratory conditions, WJ-MSC took 25 ± 5 days to migrate from cord segments, adhere, and reach confluence. In subsequent passages (up to P4) the confluence time was halved in each passage and the confluent cell counts reached to 5×10^6 cells/mL. Flow cytometric analysis of WJ-MSC from passage 3, 4, and 5 (before and after freezing) revealed (>95%) from each passage, and were positive for the mesenchymal markers CD29, CD105, CD90, CD73, whereas 74.9% were positive for CD44. Less than 2% of the cells showed positivity to the hematopoietic markers CD34, CDHLA-DR, CD14, CD19, and CD45 (Fig. 1). In addition, the cells were able to differentiate into trilineage mesenchymal cells such as adipocytes, chondrocytes, and osteocytes when induced (data not shown).

Confluent HUVEC (P2, P3) monolayers expressed VE-cadherin at cell–cell contacts. The pattern of staining was predominantly continuous (>90% of cell–cell borders; Fig. 2A).

Effect of mixed media on WJ-MSC and HUVEC

PKH26-labeled WJ-MSC displayed no alteration in morphology and retained the dye over an observed 10 days. They attached to 1% gelatin-coated coverslips and grew to 70% confluence by 22 h in mixed stem cell/endothelial media. The cells displayed proliferation: at 2 h, counts revealed a mean cell density of 82 cells/mm^2, which increased to 320 cells/mm^2 at 16 h, whereas at 22 h there were on average 487 cells per mm^2 (Fig. 2D–F). The cells displayed the transition of cell shape—from rounded to intermediate to elongated spindle shaped with time over the observation period (Fig. 2D–I). They displayed negative immunoreactivity to anti-VE-cadherin antibodies (Fig. 2G–I). HUVEC also continued to show the typical cobblestone appearance and positivity to the endothelial marker before and after addition of the mixed media for the durations tested (Fig. 2A–C). Continuous VE-cadherin staining was seen in 88 + 1.6 SD% of cell–cell junctions when cells reached full confluence in mixed media.

Coculture studies

Early coculture interactions. With phase contrast microscopy, WJ-MSC were seen to attach to the HUVEC monolayer within 30 min and appeared to display morphological changes—from rounded to transitional to spindle shaped. The position of these cells in relation to the endothelial layer was difficult to decipher at the magnifications allowed. Real-time imaging (every 15 min) with a time lapse fluorescence microscope showed that soon after addition of PKH26-labeled WJ-MSC on HUVEC monolayers they displayed membrane blebbing (Fig. 3A, B) and shedding of PKH26-filled exosomes (Fig. 3C). The blebbing behavior was followed by pseudopodial extensions and amoeboid movement (Fig. 4) over HUVEC. Cells were then observed to round up and change shape toward the spindle-shaped morphology (Fig. 4). PKH26-filled exosomes were shed throughout this period.

Transmigration events. Fluorescent micrographs of immunostained cocultures from different durations showed that transmigration of cells from the apical surface to subendothelial layers started from 60 min onwards. At 2 h, $46\% \pm 11\%$ of all attached WJ-MSC were found in subendothelial locations. At 16 h, the majority of WJ-MSC ($95\% \pm 4\%$) was found in sub-endothelial position. $96\% \pm 3\%$ of WJ-MSC were found in sub-endothelial positions at 22 h.

VE-cadherin dynamics. The pattern of VE-cadherin localization was observed to differ in HUVEC monolayers with or without added PKH26-labeled WJ-MSC at 2, 16, and 22 h. Control HUVEC monolayers (no added stem cells) showed the presence of VE-cadherin at cell–cell boundaries, with a predominant continuous staining pattern at all time points (Fig. 5). In cocultures, attachment and paracellular

FIG. 5. **(A–L)** Micrographs showing localization of VE-cadherin (*green*) in HUVEC monolayers without **(A, D, G)** or with added PKH26-labeled WJ-MSC (*red*) at 2, 16, and 22 h **(B, C, E, F, H–L)**. **(A, D, G)** Control HUVEC monolayers show presence of VE-cadherin at cell–cell boundaries, with a predominant continuous staining pattern at all time points. **(B)** Image of coculture with FITC filter only showing VE-cadherin localization in HUVEC after 2 h of coculture with WJ-MSC. Cell–cell junctions with discontinuous VE-cadherin pattern or loss of staining (*arrow*) can be seen. **(C)** Superimposed images (FITC/TRITC filters) of the same area showing position of WJ-MSC (*red*) to the discontinuous cell–cell junctions. They can be seen overlying or in close association with the disrupted cell–cell borders. **(E, F)** Similar dual images at 16 h of coculture show colocalization of WJ-MSC at disrupted cell–cell junctions. **(H, I)** At 22 h of coculture, increased numbers of cell–cell borders contain a continuous VE-cadherin staining. In the merged image **(I)** WJ-MSC can be seen underlying the HUVEC monolayer. Bar = 40 μm for images **(A–I)**. **(J–L)** Merged images at higher magnification at 22 h coculture from different experimental repeats, Bar = 20 μm. Full junctional occupancy of VE-cadherin can be seen in cell–cell boundaries overlying WJ-MSC **(J)**. Sub-endothelial position of WJ-MSC can be seen in **(K)** and **(L)**. Again overlying junctions show full VE-cadherin occupancy. Note discreet shed exosomes can be seen in coculture images. **(M)** Histogram of percentage of continuous VE-cadherin junctions at different time points for control and cocultured cells. Two-way ANOVA revealed a significant decrease at 2 h ($P < 0.0001$) and significant increase at 22 h ($P < 0.001$) in the cocultures compared with control. Junctional continuity was also statistically significant at each duration of coculture ($P < 0.0001$) **(N)**. Representative western blot showing expression of VE-cadherin. PKH26-labeled WJ-MSC show negative expression (S0h, S2h, S22h) for each duration, HUVEC without WJ-MSC (E0h, E2h, E22h) show no change in expression with duration of culture whereas an upregulation of VE-cadherin can be seen in at 22 h in HUVEC cocultured with WJ-MSC (C0h, C2h, C22h). GAPDH acted as loading control. **(O)** Histogram showing mean optical density + SEM of normalized VE-cadherin expression from three different blots of control HUVEC and cocultures at 2 and 22 h. No significant changes were seen in the control groups. There was a significant upregulation of VE-cadherin expression at 22 h in the coculture group ($P < 0.01$). Color images available online at www.liebertpub.com/scd

transmigration across the endothelial layer was observed from 2 h and was concomitant with changes in VE-cadherin staining pattern to a discontinuous, stitch-like, or no staining pattern in ~35% of all cell–cell junctions. Specifically, HUVEC with overlying or transmigrating labeled WJ-MSC showed junctional disruption (Fig. 5B, C) compared with continuous VE-cadherin staining seen in HUVEC distant from WJ-MSC. A similar pattern of disruption related to stem cell proximity was seen in 16 h cocultures. The stem cells overlying HUVEC, traversing intercellular gaps and in

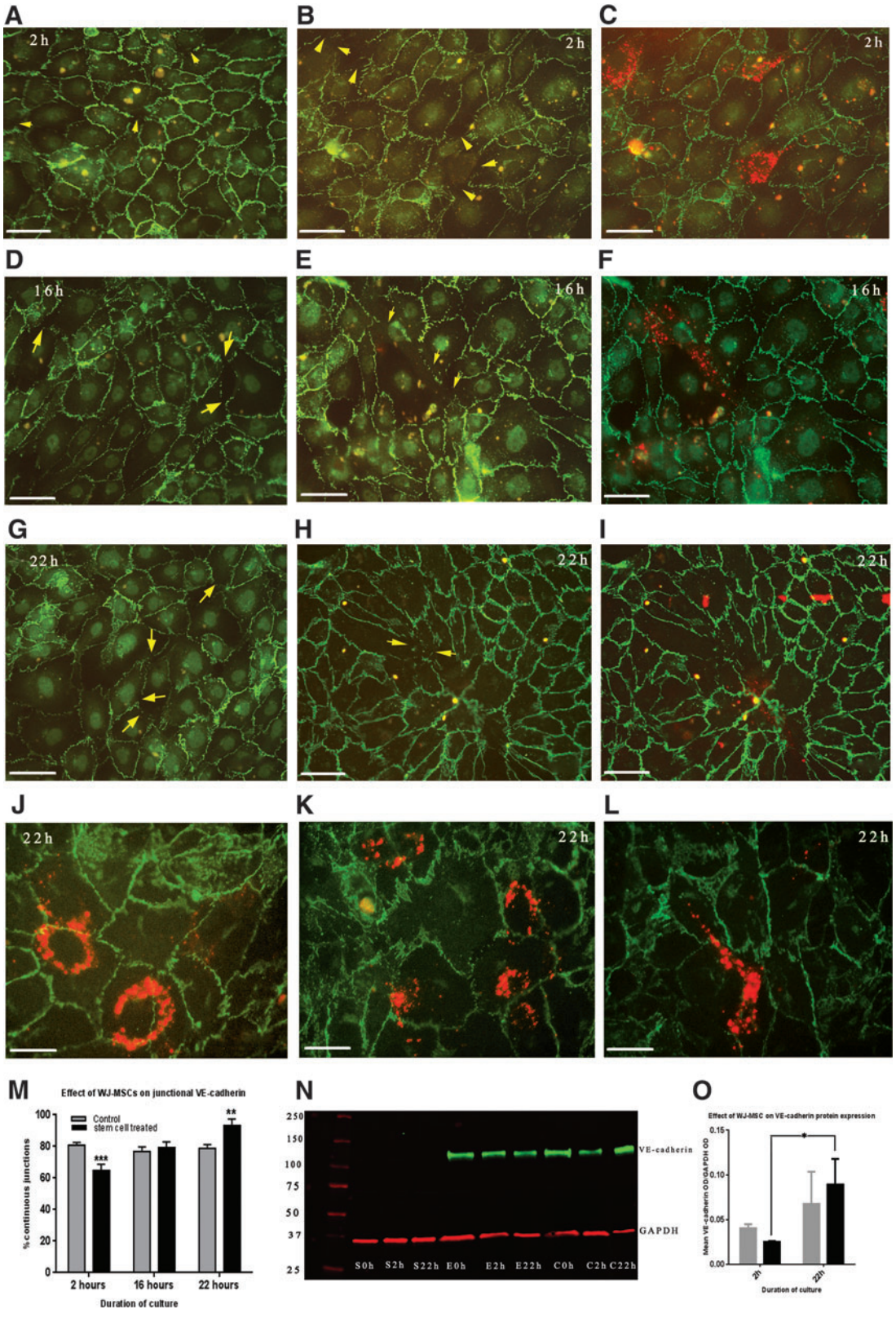

sub-endothelial positions were all immunonegative to VE-cadherin. At 22 h all WJ-MSC were observed in sub-endothelial position with overlying paracellular clefts showing full occupancy of VE-cadherin (Fig. 5J–L).

Quantitative analyses (Fig. 5M) revealed a statistically significant decrease (64.9%; $P < 0.0001$) in the percentage of cell–cell borders showing continuous VE-cadherin staining at 2 h compared to control HUVEC (80.9% ± 2.9%). At 16 h both control and treated groups had similar (76.9% ± 4.6% vs. 79.2% ± 3%) continuous junctional profiles. At 22 h, the percentage of continuous junctions were statistically higher (93.4 ± 3.2) in the WJ-MSC-treated samples versus the control (78.8% ± 3.4%; $P < 0.001$). Intraspecific comparisons of groups showed that junctional staining pattern in control HUVEC monolayers were not significantly different at 2, 16, and 22 h whereas in treated groups the percentage of continuous junctions differed at each time point of coculture ($P < 0.001$).

Western blot analyses ($n = 3$) of cocultures and control monolayers at 2 and 22 h showed that that WJ-MSC did not express VE-cadherin, whereas HUVEC showed differential expression dependent on treatment and duration of stem cell interaction (Fig. 5N). Statistical analysis revealed no significant change in VE-cadherin values (normalized against GAPDH) in the control groups from 2 to 22 h, whereas the cocultures showed significant upregulation of VE-cadherin protein in the same time interval ($P \leq 0.01$; Fig. 5O). This intraspecific difference corresponded with junctional changes seen by immunofluorescence analyses.

Confocal microscopy of cocultures, immunostained with VE-cadherin and tilting at the Z axis confirmed attachment and paracellular transmigration of WJ-MSC across the endothelial layer at 2 h, (Fig. 6A–D). Furthermore, Z-tilts confirmed basal position of all stem cells at 22 h (Fig. 6E–G). The endothelial cell–cell junctions showed the continuous VE-cadherin pattern above the transmigrated stem cells.

Discussion

This study showed that human MSCs isolated from the umbilical cord can cross the endothelial barrier without causing endothelial damage. The transmigration appeared to be similar to that shown for bone marrow stem cell migration [4], taking a period of hours rather than minutes. WJ-MSC demonstrated nonapoptotic blebbing upon addition, amoeboid motility, changes in cell shape, and paracellular transmigration to the sub-endothelial layer. Our data also suggests that WJ-MSC can influence junctional expression of the paracellular adhesion molecule VE-cadherin, with VE-cadherin perturbation as an early event followed by transmigration and a full return of VE-cadherin to junctional domains. Indeed, once WJ-MSC were in the sub-endothelial niche, they appeared to upregulate both VE-cadherin protein expression and their occupancy at HUVEC–cell borders.

Exposure of PH26-labeled WJ-MSC to 50% endothelial media did not alter their ability to attach, proliferate, grow to confluence, and retain the dye (Fig. 2). They did not demonstrate phenotypic alteration toward the endothelial lineage—they continued to be negative for VE-cadherin when grown in mixed media or when cocultured with HUVEC. Addition of 50% stem cell media to HUVEC at near confluence did not alter its ability to reach full confluence within 24 h. Junctional maturity (as evidenced by continuous VE-cadherin staining) and vWF expression was similar to that seen in HUVEC grown in 100% endothelial medium. There were no statistically significant differences in the percentage of junctions showing continuous VE-cadherin at 2, 16, or 22 h in mixed media alone (control; Fig. 5). In cocultures there was a significant upregulation of total protein in HUVEC after 96% of WJ-MSC had transmigrated to the adluminal (sub-endothelial) position. This increase was due to the changes in HUVEC since WJ-MSC remains immunonegative for VE-cadherin at all durations of coculture (Fig. 5N). However, where VE-cadherin resides, junctional occupancy rather than cytoplasmic location, dictates barrier integrity [6]. Thus the observed changes in junctional VE-cadherin staining with duration of coculture were revealing (Fig. 5). The statistically significant increase in disruption of the VE-cadherin AJs in the HUVEC monolayer was an early event and peaked at 2 h after introduction of WJ-MSC (Fig. 5). Transendothelial migration of WJ-MSC started from 60 min and ~46% of cells had transmigrated by 2 h. Return of VE-cadherin and full junctional occupancy was a postmigratory event, starting around 16 h and reaching a higher percentage continuous than control HUVEC monolayers at 22 h. VE-cadherin protein expression was at its highest at this point.

The discreet but significant perturbations of HUVEC–cell borders, which started from 60 min are reminiscent of that seen for vasoactive agents such as VEGF and histamine [13,14]. These inflammatory mediators have a biphasic response with rapid transendothelial pore formation (minutes) followed by a paracellular distension after 30–60 min [15–17]. The delayed interaction we observed argues toward VE-cadherin relocation to facilitate transmigration. BM-MSC have been shown to migrate through the paracellular pathway of human brain micro-VE cell monolayers, through the disruption of ZO-1 and occludin and alteration of tight junction integrity [18]. The postmigratory return of VE-cadherin in our cocultures agrees with other studies. Pati et al. showed that BM-MSC can reduce HUVEC monolayers permeability in vitro after 24 h with enhanced VE-cadherin/β-catenin interactions [12]. Menge et al. showed that BM-MSC inhibit HUVEC proliferation and angiogenesis after 2 days of coculture through the modulation of VE-cadherin/β-catenin signaling pathway [19]. Our studies show that umbilical mesenchymal cells have a similar ability; moreover we show that this is preceded by paracellular VE-cadherin disruption during transmigration. The return of VE-cadherin and HUVEC confluence seems to be related to a paracrine conversation between WJ-MSC and HUVEC. According to [20] WJ-MSC can stimulate neovascularization by secreting paracrine factors and by acting as perivascular precursor cells. The observed shedding of exosomes before transmigration suggests that exosomal signaling may also be an early event (Figs. 3 and 4). Released exosomes from placental mesenchymal cells have been shown to have a dose-dependent effect on migration and tube formation of placental micro-VE cells [21]. Whether exosomal signaling can induce junctional disruption requires investigation and is underway in our laboratory.

Our real-time studies (Figs. 3 and 4) revealed that transmigration is not an all or nothing event, with all added cells

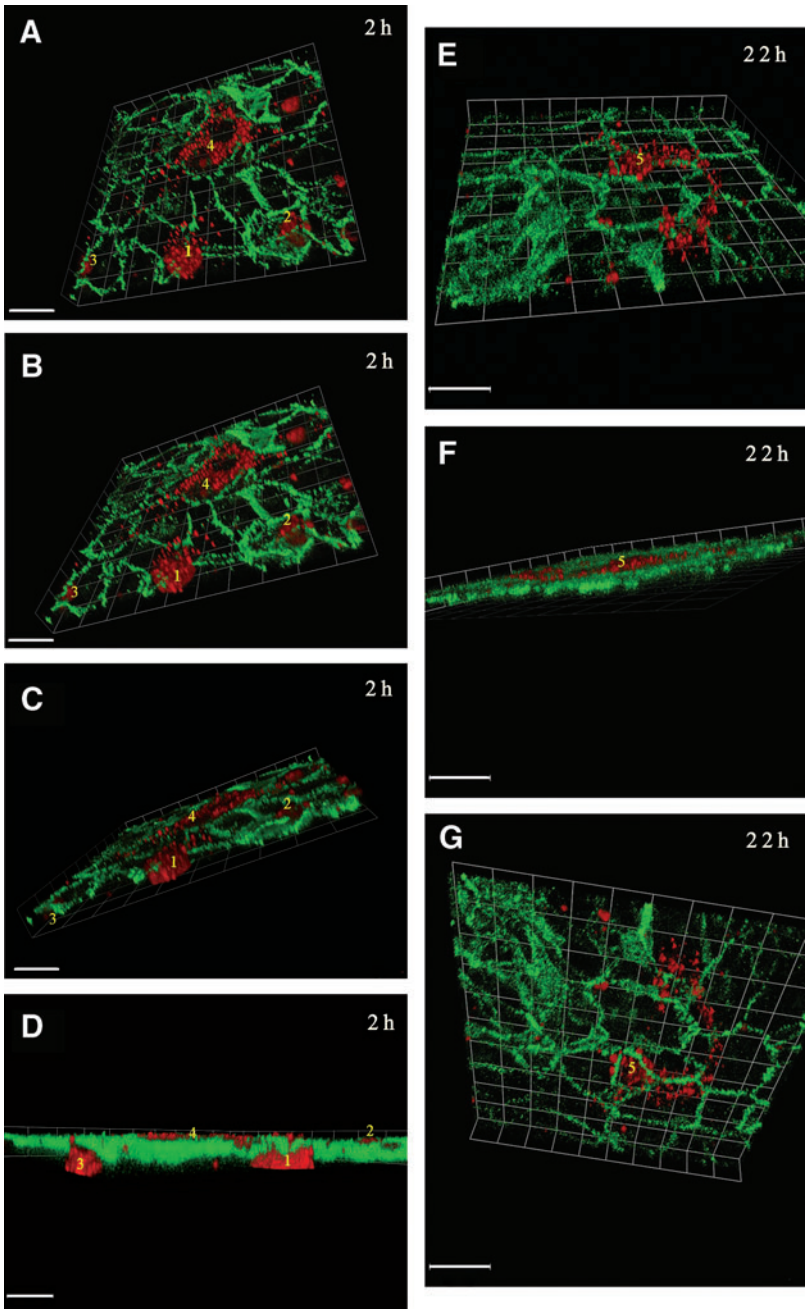

FIG. 6. **(A–G)** Confocal composite micrographs of optical sections. **(A–D;** 22 slices at 0.5 μm intervals and **E–G;** 10 slices at 0.6 μm intervals) of PKH26 (*red*)-labeled WJ-MSC cocultured with VE-cadherin (*green*)-labeled HUVEC, where VE-cadherin clearly demarcates cell–cell contact regions of the monolayer. Images were tilted on the Z-axis at varying angles with the Volocity Software, starting from the sub-endothelial position. **(A, B)** At 2 h coculture, three WJ-MSC (1, 2, 3) can be seen traversing at cell–cell borders, where VE-cadherin staining is disrupted or absent. Cell 4 is seen fully attached and spread under the HUVEC monolayer. **(C, D)** confirms the paracellular transmigrating of cells 1–3. Bar = 120 μm. **(E–G)** Confocal micrographs of optical sections of cocultures at 22 h, tilted with Volocity software, starting from a sub-endothelial position; Bar = 100 μm. **(E, F)** Elongated spindle-shaped WJ-MSC (5) can be seen under the HUVEC monolayer traversing over several cells. Tilting to the apical surface of the monolayer **(G)** demonstrates repair of the junctional regions with full occupancy of VE-cadherin (continuous staining) in paracellular clefts overlying the stem cell (5). Color images available online at www.liebertpub.com/scd

transmigrating soon after addition. Increasing number of WJ-MSC crossed the endothelial barriers over the 24 h observation period, with migration starting around 60 min. Forty-six percent of attached cells crossed in the first 2 h and the remainder continued crossing up to the 24 h. The initial lag phase and prolonged duration is similar to an in vivo study of the perfused mouse heart, where Schmidt et al. reported that 50% of introduced bone marrow stem cells migrated through the endothelial barrier within 60 min perfusion [5]. We did not see any reverse trafficking of migrated cells. Once the sub-endothelial position was reached, cells attached and became quiescent. This may be the consequence of improved adhesion of WJ-MSC on gelatin. In our study we used isolated MSCs from the incised umbilical cord. These cells showed essential MSC characteristics such as plastic adherence, tripotency, and expression of CD29, CD105, CD90, CD73, and CD44. However, heterogeneous populations of MSCs, both in origin (pericytic or fibroblastic) and differentiation potency is now a hotly discussed topic [22] and may explain the reported vascular repair potential of MSCs. Of the 20,000 WJ-MSC added to each endothelial-lined well and grown in mixed media, only a proportion ($\sim$50%) of the added stem cells crossed the endothelial barrier. The ability of this cohort to survive (adapt) in 50% endothelial media and their preference for the sub-endothelial niche is suggestive of the existence of cells with different lineage potential in the >96% pure characterized MSCs. Thus these stem cells may be more amenable to perivascular lineage commitment. Indeed the subsequent maturation of endothelial VE-cadherin

junctions seen in HUVEC at 22 h coculture mimics an endothelial-pericyte cross-talk and gives credence to this hypothesis.

The blebbing behavior of the WJ-MSC upon introduction was observed not to be an apoptotic phenomenon. The very same cells were then seen to display amoeboid movement and change shape (Fig. 4). This type of membrane changes after trypsinization of adhered cells and addition to new extracellular matrix has been shown for cells; indeed bled-mediated migration for navigation and mechanical homeostasis is a critical cellular activity [23]. Teo et al. [4] also attributed blebbing of bone marrow stem cells to low avidity interaction between endothelium and MSC, whereas quenching of blebbing may be promoted by contact with the sub-endothelial matrix after transmigration. WJ-MSC in our study showed exactly the same response in their search for new optimal attachment sites at the sub-endothelial niches (Figs. 3 and 4). As stated before, in our study, confocal microscopy and Z-tilting indicate that emigration sites for WJ-MSC were at cell–cell contact regions (Fig. 6). Transcellular migration was not observed, but cannot be excluded. The time taken to transmigrate was similar to that seen for bone marrow stem cells rather than leucocytes [24].

In conclusion, this study is the first to show the early events of transmigration of WJ-MSC isolated from the human umbilical cord through HUVEC. Our data adds strength to the observations that alteration in VE-cadherin localization at junctional domains accompanies MSC migration to perivascular regions. The traffic to sub-endothelial regions and influence on endothelial integrity and VE-cadherin occupancy suggest that WJ-MSC have an important perivascular/pericytic function, in general, and throughout gestation, in particular.

Acknowledgments

The authors wish to thank the staff and patients of Labor Suite, Queens Medical Centre, Nottingham for their help and generosity. The authors thank Dr. Emma King, Advanced Imaging Unit, for her advice on real-time imaging. The DeltaVision Microscope used was funded by the Wellcome Trust, 094233/Z/10/Z. Thanks also to the Islamic Development Bank (IDB) for funding the PhD studentship of N.E.

Data from this article was presented as a poster in British Microcirculation Society's annual meeting in University of Bristol, April 2014.

Author Disclosure Statement

No competing financial interests exist.

References

1. Kobayashi K, T Kubota and T Aso. (1998). Study on myofibroblast differentiation in the stromal cells of Wharton's jelly: expression and localization of alpha-smooth muscle actin. Early Hum Dev 51:223–233.
2. Fan CG, QJ Zhang and JR Zhou. (2011). Therapeutic potentials of mesenchymal stem cells derived from human umbilical cord. Stem Cell Rev 7:195–207.
3. Sokolova IB, NN Zin'kova, EV Shvedova, PV Kruglyakov and DG Polyntsev. (2007). Distribution of mesenchymal stem cells in the area of tissue inflammation after transplantation of the cell material via different routes. Bull Exp Biol Med 143:143–146.
4. Teo GS, JA Ankrum, R Martinelli, SE Boetto, K Simms, TE Sciuto, AM Dvorak, JM Karp and CV Carman. (2012). Mesenchymal stem cells transmigrate between and directly through tumor necrosis factor-alpha-activated endothelial cells via both leukocyte-like and novel mechanisms. Stem Cells 30:2472–2486.
5. Schmidt A, D Ladage, C Steingen, K Brixius, T Schinkothe, FJ Klinz, RH Schwinger, U Mehlhorn and W Bloch. (2006). Mesenchymal stem cells transmigrate over the endothelial barrier. Eur J Cell Biol 85:1179–1188.
6. Dejana E, F Orsenigo and MG Lampugnani. (2008). The role of adherens junctions and VE-cadherin in the control of vascular permeability. J Cell Sci 121:2115–2122.
7. De Bruyn C, M Najar, G Raicevic, N Meuleman, K Pieters, B Stamatopoulos, A Delforge, D Bron and L Lagneaux. (2011). A rapid, simple, and reproducible method for the isolation of mesenchymal stromal cells from Wharton's jelly without enzymatic treatment. Stem Cells Dev 20:547–557.
8. Dominici M, K Le Blanc, I Mueller, I Slaper-Cortenbach, F Marini, D Krause, R Deans, A Keating, Dj Prockop and E Horwitz. (2006). Minimal criteria for defining multipotent mesenchymal stromal cells. The International Society for Cellular Therapy position statement. Cytotherapy 8:315–317.
9. Pittenger MF, AM Mackay, SC Beck, RK Jaiswal, R Douglas, JD Mosca, MA Moorman, DW Simonetti, S Craig and DR Marshak. (1999). Multilineage potential of adult human mesenchymal stem cells. Science 284:143–147.
10. Santos JM, RN Barcia, SI Simoes, MM Gaspar, S Calado, A Agua-Doce, SC Almeida, J Almeida, M Filipe, et al. (2013). The role of human umbilical cord tissue-derived mesenchymal stromal cells (UCX(R)) in the treatment of inflammatory arthritis. J Transl Med 11:18.
11. Hamilton RD and L Leach. (2011). Isolation and properties of an in vitro human outer blood-retinal barrier model. Methods Mol Biol 686:401–416.
12. Pati S, AY Khakoo, J Zhao, F Jimenez, MH Gerber, M Harting, JB Redell, R Grill, Y Matsuo, et al. (2011). Human mesenchymal stem cells inhibit vascular permeability by modulating vascular endothelial cadherin/beta-catenin signaling. Stem Cells Dev 20:89–101.
13. Esser S, MG Lampugnani, M Corada, E Dejana and W Risau. (1998). Vascular endothelial growth factor induces VE-cadherin tyrosine phosphorylation in endothelial cells. J Cell Sci 111:1853–1865.
14. Leach L, BM Eaton, ED Westcott and JA Firth. (1995). Effect of histamine on endothelial permeability and structure and adhesion molecules of the paracellular junctions of perfused human placental microvessels. Microvasc Res 50:323–337.
15. Absi M, JI Bruce and DT Ward. (2014). The inhibitory effect of simvastatin and aspirin on histamine responsiveness in human vascular endothelial cells. Am J Physiol Cell Physiol 306:C679–C686.
16. Bates DO. (2010). Vascular endothelial growth factors and vascular permeability. Cardiovasc Res 87:262–271.
17. Wegener J and J Seebach. (2014). Experimental tools to monitor the dynamics of endothelial barrier function: a survey of in vitro approaches. Cell Tissue Res 355:485–514.

18. Lin MN, DS Shang, W Sun, B Li, X Xu, WG Fang, WD Zhao, L Cao and YH Chen. (2013). Involvement of PI3K and ROCK signaling pathways in migration of bone marrow-derived mesenchymal stem cells through human brain microvascular endothelial cell monolayers. Brain Res 1513:1–8.
19. Menge T, M Gerber, K Wataha, W Reid, S Guha, CS Cox, Jr., P Dash, MS Reitz, Jr., AY Khakoo and S Pati. (2013). Human mesenchymal stem cells inhibit endothelial proliferation and angiogenesis via cell-cell contact through modulation of the VE-Cadherin/beta-catenin signaling pathway. Stem Cells Dev 22:148–157.
20. Choi M, HS Lee, P Naidansaren, HK Kim, E O, JH Cha, HY Ahn, PI Yang, JC Shin and YA Joe. (2013). Proangiogenic features of Wharton's jelly-derived mesenchymal stromal/stem cells and their ability to form functional vessels. Int J Biochem Cell Biol 45:560–570.
21. Salomon C, J Ryan, L Sobrevia, M Kobayashi, K Ashman, M Mitchell and GE Rice. (2013). Exosomal signaling during hypoxia mediates microvascular endothelial cell migration and vasculogenesis. PLoS One 8:e68451.
22. Lv FJ, RS Tuan, KM Cheung and VY Leung. (2014). The surface markers and identity of human mesenchymal stem cells. Stem Cells 32:1408–1419.
23. Norman LL, J Brugues, K Sengupta, P Sens and H Aranda-Espinoza. (2010). Cell blebbing and membrane area homeostasis in spreading and retracting cells. Biophys J 99:1726–1733.
24. Stock C and C Riethmuller. (2011). Endothelial activation drives lateral migration and diapedesis of leukocytes. Cell Immunol 271:180–183.

Address correspondence to:
Prof. Lopa Leach
Cardiovascular Research Group
School of Life Sciences
Faculty of Medicine & Health Sciences
University of Nottingham
E Floor Medical School
Queens Medical Centre
Nottingham NG7 2UH
United Kingdom

E-mail: lopa.leach@nottingham.ac.uk

Received for publication April 28, 2014
Accepted after revision October 15, 2014
Prepublished on Liebert Instant Online XXXX XX, XXXX